Ocean Modelling 125 (2018) 39–44

Contents lists available at ScienceDirect

Ocean Modelling

journal homepage: www.elsevier.com/locate/ocemod

Short communication

A parameterization of the passive layer of a quasigeostrophic flow in a continuously-stratified ocean

E.S. Benilov[1]

Department of Mathematics and Statistics, University of Limerick, V94 T9PX, Ireland

ARTICLE INFO

Keywords:
Mesoscale flows
Quasigeostrophic approximation
Stratification

ABSTRACT

This paper examines quasigeostrophic flows in an ocean that can be subdivided into an upper active layer (AL) and a lower passive layer (PL), with the flow and density stratification mainly confined to the former. Under this assumption, an asymptotic model is derived parameterizing the effect of the PL on the AL. The model depends only on the PL's depth, whereas its Väisälä–Brunt frequency turns out to be unimportant (as long as it is small). Under an additional assumption—that the potential vorticity field in the PL is well-diffused and, thus, uniform—the derived model reduces to a simple boundary condition. This condition is to be applied at the AL/PL interface, after which the PL can be excluded from consideration.

1. Introduction

Oceanic currents and density stratification are often confined to an upper active layer (AL) of the ocean, which does not, however, mean that the response of the lower passive layer (PL) can be neglected. As a result, a significant proportion of computer resources in numerical simulations has to be spent on the PL—even if/when nothing significant occurs there in the problem at hand.

The high cost of resolving the PL is not the only difficulty when modeling a layered ocean. Since little is known about the Väisälä–Brunt frequency N in the ocean's deeper parts (except that N is small), modeling the PL poses problems even if one has resources for resolving it. An additional difficulty arises when one uses the quasigeostrophic (QG) model, which becomes singular in the limit $N \to 0$. To avoid all these problems, many assume the Väisälä–Brunt frequency to be constant—which is, however, not the case near the AL/PL interface and, thus, may give rise to an error which is impossible to estimate.

In this work, a model is presented, parameterizing the effect of the passive layer on the active layer under the QG approximation. The problem is formulated in Section 2, solved asymptotically in Section 3, and Section 4 addresses the practical issue of how one can subdivide a *continuously* stratified ocean into an AL and PL. In Section 5, the general asymptotic model is adapted for the case where the potential vorticity field in the PL is uniform.

2. The governing equations

Consider a mesoscale flow in the ocean characterized by the Coriolis parameter f and the Väisälä–Brunt frequency $N(z)$, where z is the vertical coordinate (with (x, y) and t being the horizontal coordinates and time). Let the flow be described by the QG equation for the stream function ψ (for the applicability of the QG theory, see Pedlosky, 1987),

$$\frac{\partial}{\partial t}\left[\nabla^2\psi + \frac{\partial}{\partial z}\left(\frac{f^2}{N^2}\frac{\partial\psi}{\partial z}\right)\right] + J\left[\psi,\, \nabla^2\psi + \frac{\partial}{\partial z}\left(\frac{f^2}{N^2}\frac{\partial\psi}{\partial z}\right)\right] = 0, \tag{1}$$

where the (horizontal) Laplacian and Jacobian are

$$\nabla^2\psi = \frac{\partial^2\psi}{\partial x^2} + \frac{\partial^2\psi}{\partial y^2}, \qquad J\,[\psi,\, Q] = \frac{\partial\psi}{\partial x}\frac{\partial Q}{\partial y} - \frac{\partial\psi}{\partial y}\frac{\partial Q}{\partial x}.$$

Under the rigid-lid approximation, the boundary conditions at the ocean's surface and bottom are

$$\frac{\partial^2\psi}{\partial t\,\partial z} + J\left[\psi,\, \frac{\partial\psi}{\partial z}\right] = 0 \qquad \text{at} \qquad z = 0, \tag{2}$$

$$\frac{\partial^2\psi}{\partial t\,\partial z} + J\left[\psi,\, \frac{\partial\psi}{\partial z}\right] = 0 \qquad \text{at} \qquad z = -H, \tag{3}$$

where H is the ocean's depth.

3. The analysis

Assume that the ocean can be subdivided into an active and passive layers, of depths H_a and $H_p = H - H_a$, with the corresponding scales of the Väisälä–Brunt frequency being such that $N_a \gg N_p$. Introduce also the horizontal spatial scale L of the flow (the same for both AL and PL).

E-mail address: Eugene.Benilov@ul.ie.
[1] http://www.staff.ul.ie/eugenebenilov/hpage/.

https://doi.org/10.1016/j.ocemod.2018.03.003
Received 7 December 2017; Received in revised form 5 March 2018; Accepted 22 March 2018
Available online 30 March 2018
1463-5003/

Now, two Burger numbers can be introduced,

$$Bu_a = \frac{N_a^2 H_a^2}{f^2 L^2}, \qquad Bu_p = \frac{N_p^2 H_p^2}{f^2 L^2}.$$

The only assumption used in this work is that Bu_p is small[2] (mainly due to the smallness of N_p), whereas Bu_a remains unrestricted.

The following derivation is straightforward, so there is no need to nondimensionalize the governing equations. If $Bu_p \ll 1$, the terms involving $1/N^2$ dominate Eq. (1) in the PL, so that the solution of (1) can be sought in the form of a series,

$$\psi = \psi^{(0)} + \psi^{(1)} + \cdots \qquad \text{for} \qquad z \in (-H, -H_a),$$

where $\psi^{(1)}/\psi^{(0)} = \mathcal{O}(Bu_p)$ and

$$\frac{\partial^2}{\partial t\, \partial z}\left(\frac{f^2}{N^2}\frac{\partial \psi^{(0)}}{\partial z}\right) + J\left[\psi^{(0)}, \frac{\partial}{\partial z}\left(\frac{f^2}{N^2}\frac{\partial \psi^{(0)}}{\partial z}\right)\right] = 0, \tag{4}$$

$$\frac{\partial}{\partial t}\left[\nabla^2\psi^{(0)} + \frac{\partial}{\partial z}\left(\frac{f^2}{N^2}\frac{\partial \psi^{(1)}}{\partial z}\right)\right] + J\left[\psi^{(1)}, \frac{\partial}{\partial z}\left(\frac{f^2}{N^2}\frac{\partial \psi^{(0)}}{\partial z}\right)\right] + J\left[\psi^{(0)}, \nabla^2\psi^{(0)} + \frac{\partial}{\partial z}\left(\frac{f^2}{N^2}\frac{\partial \psi^{(1)}}{\partial z}\right)\right] = 0. \tag{5}$$

Note that a two-layer, beta-plane equivalent of Eq. (4) has been previously derived by Dewar and Gailliard (1994).

The boundary condition (3), in turn, yields

$$\frac{\partial^2\psi^{(0)}}{\partial t\, \partial z} + J\left[\psi^{(0)}, \frac{\partial \psi^{(0)}}{\partial z}\right] = 0 \qquad \text{at} \qquad z = -H, \tag{6}$$

$$\frac{\partial^2\psi^{(1)}}{\partial t\, \partial z} + J\left[\psi^{(0)}, \frac{\partial \psi^{(1)}}{\partial z}\right] + J\left[\psi^{(1)}, \frac{\partial \psi^{(0)}}{\partial z}\right] = 0 \qquad \text{at} \qquad z = -H. \tag{7}$$

Next, to match the PL and AL solutions, one should require the continuity of the pressure and isopycnal displacement. Under the QG approximation, this amounts to

$$(\psi)_{z=-H_a-0} = (\psi)_{z=-H_a+0}, \qquad \left(\frac{f^2}{N^2}\frac{\partial \psi}{\partial z}\right)_{z=-H_a-0} = \left(\frac{f^2}{N^2}\frac{\partial \psi}{\partial z}\right)_{z=-H_a+0}. \tag{8}$$

Since the PL part of the streamfunction is now subdivided into $\psi^{(0)}$ and $\psi^{(1)}$, (8) should also be subdivided into two pairs of matching conditions, for $\psi^{(0)}$ and $\psi^{(1)}$,

$$(\psi^{(0)})_{z=-H_a-0} = (\psi)_{z=-H_a+0}, \qquad \left(\frac{f^2}{N^2}\frac{\partial \psi^{(0)}}{\partial z}\right)_{z=-H_a-0} = 0, \tag{9}$$

$$(\psi^{(1)})_{z=-H_a-0} = 0, \qquad \left(\frac{f^2}{N^2}\frac{\partial \psi^{(1)}}{\partial z}\right)_{z=-H_a-0} = \left(\frac{f^2}{N^2}\frac{\partial \psi}{\partial z}\right)_{z=-H_a+0}. \tag{10}$$

Observe that the AL pressure (which can be large) is matched to $\psi^{(0)}$, whereas the AL isopycnal displacement (which is relatively small as $H_a/H_p \ll 1$) is matched to $\psi^{(1)}$. This way, the 'subdivided' matching conditions are balanced, i.e., involve terms of the same order.

It turns out that $\psi^{(1)}$ can be eliminated. Integrating Eq. (5) with respect to z from $-H$ to $-H_a - 0$ and integrating by parts the terms that involve both $\psi^{(0)}$ and $\psi^{(1)}$, one can verify that the bulk (integral) terms involving $\psi^{(1)}$ cancel out and (5) becomes

$$\begin{aligned}
&\frac{\partial}{\partial t}\left[\int_{-H}^{-H_a}\nabla^2\psi^{(0)}\mathrm{d}z + \left(\frac{f^2}{N^2}\frac{\partial \psi^{(1)}}{\partial z}\right)_{z=-H_a-0} - \left(\frac{f^2}{N^2}\frac{\partial \psi^{(1)}}{\partial z}\right)_{z=-H}\right] \\
&+ \left(J\left[\psi^{(0)}, \frac{f^2}{N^2}\frac{\partial \psi^{(1)}}{\partial z}\right] + J\left[\psi^{(1)}, \frac{f^2}{N^2}\frac{\partial \psi^{(0)}}{\partial z}\right]\right)_{z=-H_a-0} \\
&- \left(J\left[\psi^{(0)}, \frac{f^2}{N^2}\frac{\partial \psi^{(1)}}{\partial z}\right] + J\left[\psi^{(1)}, \frac{f^2}{N^2}\frac{\partial \psi^{(0)}}{\partial z}\right]\right)_{z=-H} \\
&+ \int_{-H}^{-H_a} J\left[\psi^{(0)}, \nabla^2\psi^{(0)}\right]\mathrm{d}z = 0.
\end{aligned} \tag{11}$$

Now, taking into account the boundary/matching conditions (6)–(7) and (9)–(10), one obtains

$$\frac{\partial}{\partial t}\left(\nabla^2\int_{-H}^{-H_a}\psi^{(0)}\mathrm{d}z + \Phi\right) + \int_{-H}^{-H_a} J\left[\psi^{(0)}, \nabla^2\psi^{(0)}\right]\mathrm{d}z + J\left[\Psi, \Phi\right] = 0, \tag{12}$$

where

$$\Psi(x, y, t) = (\psi)_{z=H_a+0}, \qquad \Phi(x, y, t) = \left(\frac{f^2}{N^2}\frac{\partial \psi}{\partial z}\right)_{z=-H_a+0}. \tag{13}$$

The leading-order solution $\psi^{(0)}$, in turn, cannot be eliminated. Note, however, that the *passive* layer is not supposed to have independent dynamics, but should be driven by the *active* layer—i.e. the pressure field in the former, $\psi^{(0)}$, should be fully determined by the pressure applied at the interface—hence,

$$\psi^{(0)} = \Psi(x, y, t). \tag{14}$$

Subject to (14), Eqs. (4) and (6) are satisfied identically, whereas (12) yields

$$\frac{\partial}{\partial t}(H_p\nabla^2\Psi + \Phi) + J\left[\Psi, H_p\nabla^2\Psi + \Phi\right] = 0. \tag{15}$$

Note that letting $\psi^{(0)}$ be independent of z makes the PL flow barotropic, but the isopycnal displacement—determined by $(f^2/N^2)(\partial\psi^{(1)}/\partial z)$—does depend on z and is order-one (due to the presence of the factor $1/N^2$).

Thus, the complete governing set comprises:

1. the AL Eqs. (1)–(2),
2. the PL Eq. (15), and
3. the matching conditions (13), where the " $\pm$ 0" can be omitted:

$$\psi = \Psi, \qquad \frac{f^2}{N^2}\frac{\partial \psi}{\partial z} = \Phi \qquad \text{at} \qquad z = -H_a. \tag{16}$$

Items (2)–(3) are the main results of this work. Note that an approximation similar to (15)–(16) has been derived by Benilov (1995) for the particular case of normal modes in a baroclinic current. The possibility of an extension to *arbitrary* QG flows, however, was overlooked.

4. Examples

The asymptotic model developed above is valid when the ocean can be subdivided into an AL and PL. The real ocean, however, is *continuously* stratified, with no clear-cut inter-layer boundary—leaving us with a question: what is the optimal choice for the AL/PL interface?

This issue is clarified below by applying the general model (15)–(16) to the example of baroclinic instability of a vertically sheared but horizontally uniform flow. The asymptotic results for different values of H_a are then compared to the exact solution.

It is convenient to nondimensionalize the problem by introducing

[2] Note that, despite the smallness of Bu_p (which often signals that the QG approximation should be replaced with the frontal-geostrophic one), the deviation of the isopycnals in the PL is assumed small—hence, the QG still holds.

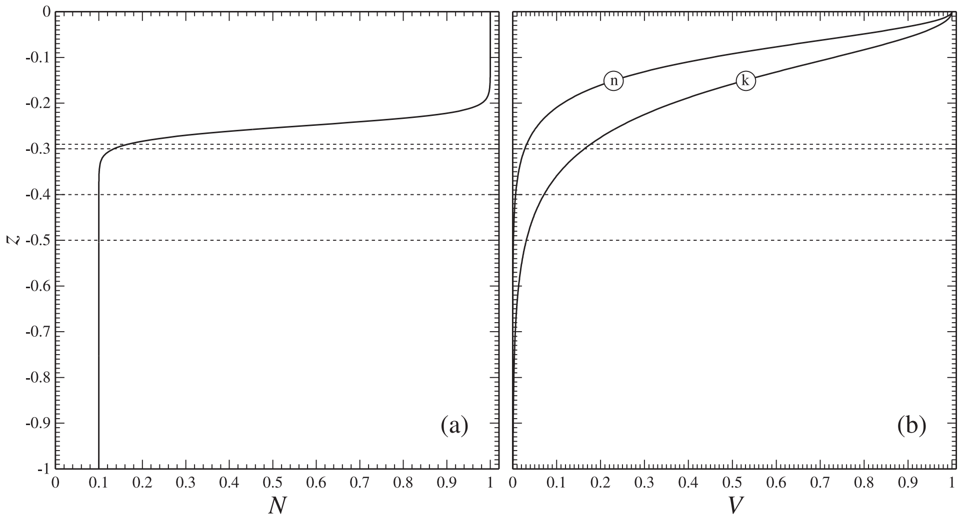

Fig. 1. The Väisälä–Brunt frequency N and velocity V *vs.* the depth z, for flows (24)–(27). The curves corresponding to the 'thi*n*' and 'thic*k*' flows are marked with (n) and (k), respectively. The dotted lines show potential positions of the AL/PL interface (the lower three are illustrated in Fig. 3, the upper two in Fig. 4).

$$N_{nd} = \frac{N}{N_a}, \qquad (x_{nd}, y_{nd}) = \frac{(x, y)}{L}, \qquad z_{nd} = \frac{z}{H}, \qquad t_{nd} = \frac{V_0 t}{L}, \qquad \psi_{nd} = \frac{\psi}{V_0 L},$$

where N_a is the maximum Väisälä–Brunt frequency, V_a is the maximum velocity, and $L = Hf/N_a$. Rewriting the exact Eqs. (1)–(3) in terms of the non-dimensional variables and omitting the subscript $_{nd}$, one obtains

$$\frac{\partial}{\partial t}\left[\nabla^2\psi + \frac{\partial}{\partial z}\left(\frac{1}{N^2}\frac{\partial\psi}{\partial z}\right)\right] + J\left[\psi, \nabla^2\psi + \frac{\partial}{\partial z}\left(\frac{1}{N^2}\frac{\partial\psi}{\partial z}\right)\right] = 0, \tag{17}$$

$$\frac{\partial^2\psi}{\partial t\,\partial z} + J\left[\psi, \frac{\partial\psi}{\partial z}\right] = 0 \qquad \text{at} \qquad z = 0, \tag{18}$$

$$\frac{\partial^2\psi}{\partial t\,\partial z} + J\left[\psi, \frac{\partial\psi}{\partial z}\right] = 0 \qquad \text{at} \qquad z = -1. \tag{19}$$

Next, let

$$\psi = -yV(z) + \tilde{\psi}(x, z, t),$$

where $V(z)$ is the base flow and $\tilde{\psi}$ is a small perturbation. Linearizing Eqs. (17)–(19) and letting

$$\tilde{\psi} = \hat{\psi}(z)\, e^{ik(x-ct)},$$

where k and c are the perturbation's wavenumber and phase speed, one obtains

$$(c - V)\left[\frac{d}{dz}\left(\frac{1}{N^2}\frac{d\hat{\psi}}{dz}\right) - k^2\hat{\psi}\right] + \hat{\psi}\frac{d}{dz}\left(\frac{1}{N^2}\frac{dV}{dz}\right) = 0, \tag{20}$$

$$(c - V)\frac{d\hat{\psi}}{dz} + \frac{dV}{dz}\hat{\psi} = 0 \qquad \text{if} \qquad z = 0, \tag{21}$$

$$(c - V)\frac{d\hat{\psi}}{dz} + \frac{dV}{dz}\hat{\psi} = 0 \qquad \text{if} \qquad z = -1. \tag{22}$$

Repeating the same procedure (linearization, etc.) for the asymptotic equations (15)–(16) and eliminating $\hat{\Psi}$ and $\hat{\Phi}$, one obtains

$$\frac{1}{N^2}\frac{d\hat{\psi}}{dz} = \left[D_p k^2 + \frac{1}{(V - c)N^2}\frac{dV}{dz}\right]\hat{\psi} \qquad \text{if} \qquad z = -D_a, \tag{23}$$

where $D_{a,p} = H_{a,p}/H$. Condition (23) is the asymptotic alternative to the exact boundary condition (22).

Numerous examples of $V(z)$ and $N(z)$ have been examined, yielding more or less the same results. Below are described those for

$$N^2(z) = \frac{1 - n_p^2}{2}\left(\tanh\frac{z - \Delta_N}{w_N} + 1\right) + n_p^2, \tag{24}$$

where $n_p = N_p/N_a$, and Δ_N and w_N are the non-dimensional depth and width of the transitional region between the main thermocline and the weakly-stratified part of the ocean (the seasonal thermocline is neglected). Assuming that the main thermocline is $800m$ deep and the transitional region is about two times thinner (see, for example, Pedlosky, 1987, Fig. 1.3.1), then recalling that the ocean's mean depth is 4 km and finally choosing a small value for n_p on a more or less *ad hoc* basis, one obtains

$$\Delta_N = 0.25, \qquad w_N = 0.3, \qquad n_p = 0.1. \tag{25}$$

The following velocity profile will be assumed:

$$V(z) = \operatorname{sech}\left(\frac{z}{\Delta_V}\right), \tag{26}$$

where Δ_V is the flow's 'penetration depth'. The following two examples have been examined: a "thin" flow (confined to the thermocline) and a 'thick' one (partly penetrating the weakly-stratified part of the ocean),

$$\left.\begin{array}{ll}\text{thin flow:} & \Delta_V = 0.07,\\ \text{thick flow:} & \Delta_V = 0.12.\end{array}\right\} \tag{27}$$

$N(z)$ and both versions of $V(z)$ are shown in Fig. 1. The corresponding slope $\eta_y(z)$ of isopycnal surfaces and the horizontal gradient $Q_y(z)$ of potential vorticity (PV),

$$\eta_y = \frac{1}{N^2}\frac{dV}{dz}, \qquad Q_y = \frac{d}{dz}\left(\frac{1}{N^2}\frac{dV}{dz}\right),$$

are plotted in Fig. 2. Observe that, for both examples of $V(z)$, the isopycnal displacement penetrates noticeably deeper than the flow and stratification themselves.

The solution of the exact eigenvalue problem (20)–(22) and that of the asymptotic problem (20)–(21), (23) were computed using the shooting method. To avoid the singularity arising in neutrally stable cases, Eq. (20) was integrated along a path in the complex-z plane bypassing the critical level (for more details, see Boyd, 1985; Benilov and Sakov, 1999). For all values of the wavenumber k, no more than one unstable ($k\,\mathrm{Im}\,c > 0$) eigenvalue has been found, for both exact and asymptotic problems.

In Figs. 3 and 4, the asymptotic phase speed $\mathrm{Re}\,c$ and growth rate

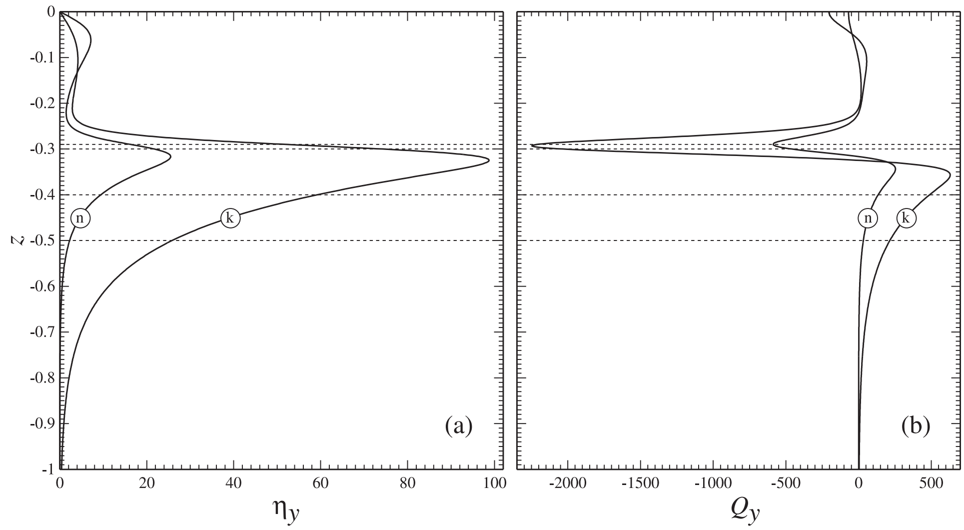

Fig. 2. The slope $\eta_y(z)$ of isopycnal surfaces and the transverse gradient $Q_y(z)$ of PV, for flows shown in Fig. 1. The labels (n) and (k) correspond to these in Fig. 1.

$k\,\mathrm{Im}\,c$ are compared to the corresponding exact results. As one might expect, a sufficiently accurate asymptotic model for the thick flow turned out to require a larger D_a than that for the thin one.

Less expectedly, the two flows turned out to differ in how the asymptotic model's accuracy improves with growing D_a. For the thick flow, it does so *gradually* – but for the thin one, the solution becomes accurate *abruptly* as soon as D_a passes a threshold of 0.3. To understand why the value of $D_a = 0.3$ is special, note that the AL/PL interface in this case is located just below the level of the extreme PV gradient—see Fig. 2 b.

More broadly, numerous examples of thin flows have been examined and the following conclusions have been drawn:

- If, for a certain choice of D_a, the AL does not include the extremum of $Q_y(z)$, the accuracy of the asymptotic model (in application to a thin flow) is poor.
- If D_a is large enough for the AL to include the extremum of $Q_y(z)$, the asymptotic model is sufficiently accurate (despite the fact that the AL may still not include the decaying portion of $Q_y(z)$ and the maximum of the isopycnal slope $\eta_y(z)$—see Fig. 2).

In the latter case, there is no point in increasing D_a beyond this threshold, as this results in wasting computational resources on a minor accuracy improvement.

For thick flows, in turn, the following 'rule of thumb' has been established: the inter-layer boundary can be drawn below the deepest

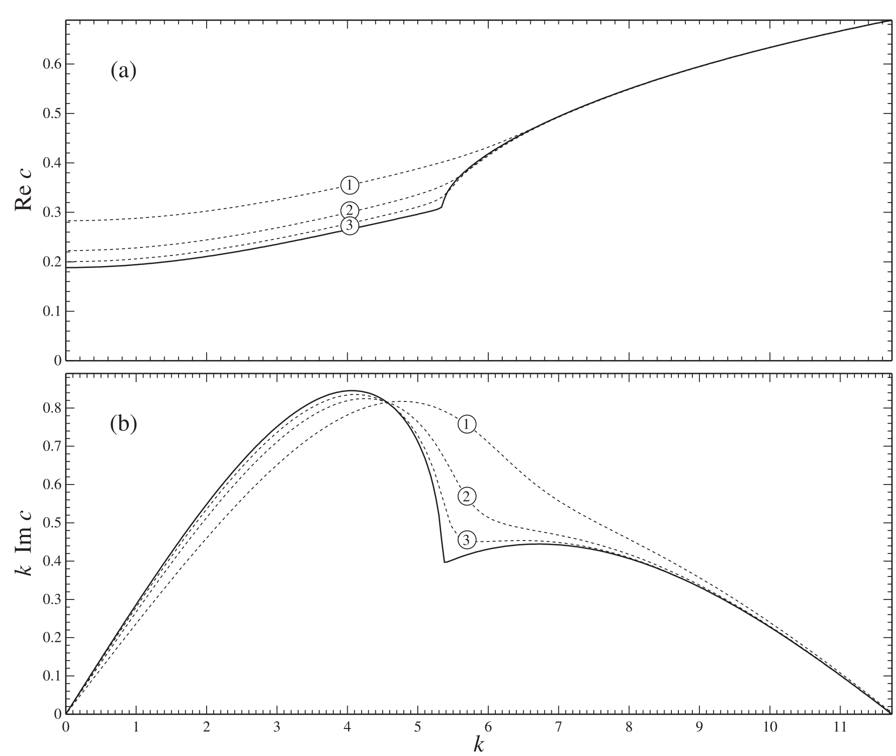

Fig. 3. The solution of the exact eigenvalue problem (20)–(22) (solid line) and that of the asymptotic problem (20)–(21), (23) with (1) $D_A = 0.3$, (2) $D_A = 0.4$, (3) $D_A = 0.5$ (dotted lines). The Väisälä–Brunt frequency N and velocity V are given by (24)–(26) with $\Delta_V = 0.12$ (thick flow). $\mathrm{Re}\,c$ is the phase speed of the disturbance and $k\,\mathrm{Im}\,c$, the growth rate.

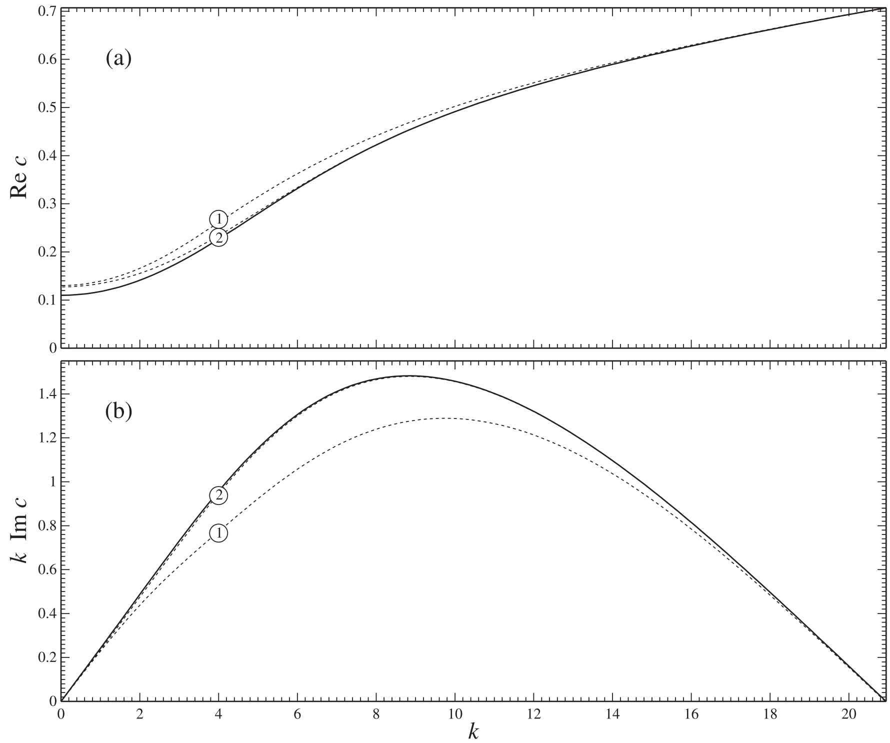

Fig. 4. The same as in Fig. 3, but for $\Delta_V = 0.07$ (thin flow) and (1) $D_A = 0.29$, (2) $D_A = 0.3$.

extremum of the PV gradient Q_y, at the depth where Q_y has decayed by a factor of 3 by comparison with that extremum. The same rule would work for thin flows as well, but it would not deliver the optimal choice in this case.

Finally, Fig. 5 illustrates the potential dangers of an often-used approach consisting in assuming $N(z)$ to be constant in the whole ocean (i.e., ignoring the PL). For thick flows, it produces noticeably less 'fitting' results than those obtained through the asymptotic model proposed. For thin flows, in turn, the two approaches produce similar results (but the asymptotic one is still 'cheaper' computationally).

5. A reduced asymptotic model

Observe that the asymptotic Eq. (15) is satisfied if

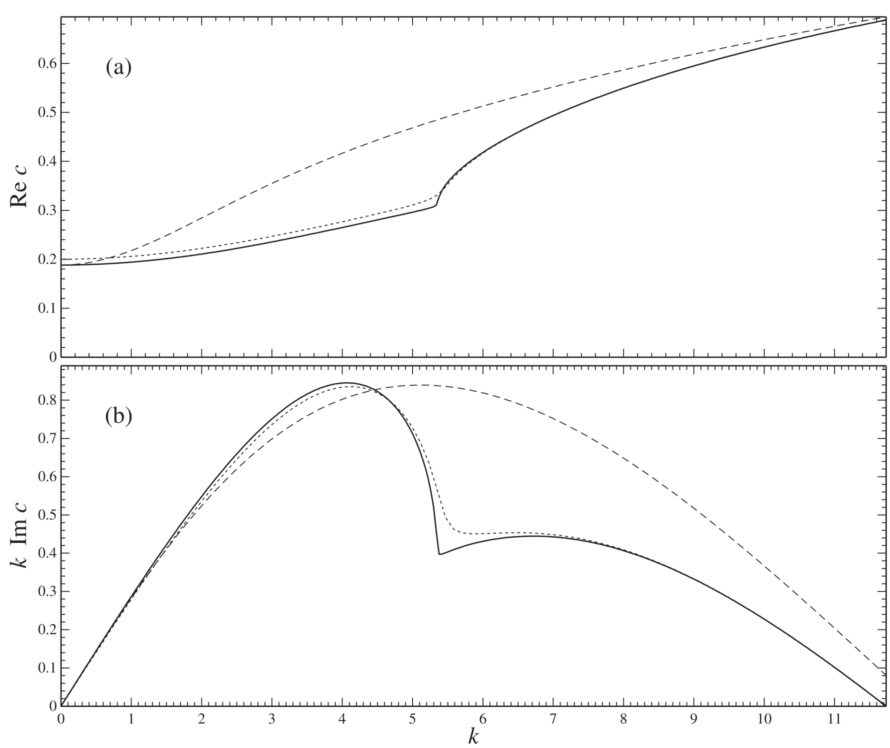

Fig. 5. The solution of the exact eigenvalue problem (20)–(22) (solid line) and that of the asymptotic problem (20)–(21), (23) with $D_A = 0.5$ (dotted line). $N(z)$ and $V(z)$ are given by (24)–(26) with $\Delta_V = 0.12$ (thick flow). The dashed line shows the solution of the exact problem (20)–(22) with $N(z) = 1$.

$$\Phi = -H_p \nabla^2 \Psi. \tag{28}$$

Reduction (28) implies that the PV anomaly in the PL is zero, i.e., the PV field itself is well-diffused—which it indeed is in the deep ocean unless up- or down-welling has recently occurred.

Substituting (28) into (16) and eliminating Ψ, one obtains

$$\frac{f^2}{N^2}\frac{\partial \psi}{\partial z} = -H_p \nabla^2 \psi \qquad \text{if} \qquad z = -H_a. \tag{29}$$

Now, one can exclude the PL from consideration and solve the (self-contained) boundary-value problem (1)–(2), (29) for the AL.

Note also that the boundary condition (29) imposes a constraint on the allowable initial condition. Consider, for example, a vertically sheared but horizontally homogeneous flow described by $\psi = -yV(z)$—which expression satisfies (29) only if

$$\frac{\mathrm{d}V}{\mathrm{d}z} = 0 \qquad \text{at} \qquad z = -H_a.$$

Another example is the so-called columnar vortices (e.g. Dritschel and de la Torre Juárez, 1996). In this case, $\psi = \psi(r)$ which satisfies (29) only if $\psi = r$ (unrestricted solid-body rotation), which is meaningless physically. In both cases, the constraint originates from the requirement of uniform potential vorticity in the PL, used to obtain the boundary condition (29).

Still, despite the constraint, the boundary condition (29) has important physical applications—e.g., near-surface oceanic vortices, which are both abundant in the ocean and crucial for its dynamics (Olson, 1991; Chelton et al., 2011). At the same time, the PV field beneath such vortices can indeed be conjectured to be uniform (Benilov, 2004; Benilov and Flanagan, 2008). In addition, a lot of work has been done on vortices submerged in a fluid with uniform PV (e.g. Dritschel et al., 2005), and (29) would be useful for extending these results to the real-ocean conditions (involving a passive layer).

It should be emphasized that the general model (15)–(16) does *not* impose any constraints on the AL initial condition.

6. Summary and concluding remarks

Thus, two models parameterizing the ocean's passive layer have been derived: the general model (15)–(16) and the reduced model (29) assuming that the PV field in the passive layer is uniform. The latter is particular simple, as it allows to fully exclude the passive layer from consideration. The former model, in turn, implies solving a partial differential equation for the passive layer—which, however, involves only horizontal spatial variables and, thus, is much simpler than the original three-dimensional QG equation. In both models, one still has to compute the solution in the active layer—but this is, of course, 'cheaper' than solving the QG equation in the whole domain.

In order to subdivide the real (continuously stratified) ocean into an AL and PL, the following 'rule of thumb' has been established: the passive layer can be assumed to begin at the depth where the horizontal PV gradient has decayed by a factor of 3 by comparison with its deepest extremum. This typically implies a reduction of the computational domain at least by 50%, and sometimes by up to 70%.

Acknowledgments

The author acknowledges the support of the Science Foundation Ireland (grant no. 12/IA/1683).

References

Benilov, E.S., 1995. Baroclinic instability of quasi-geostrophic flows localized in a thin layer. J. Fluid Mech. 288, 175–199.
Benilov, E.S., 2004. Stability of vortices in a two-layer ocean with uniform potential vorticity in the lower layer. J. Fluid Mech. 502, 207–232.
Benilov, E.S., Flanagan, J.D., 2008. The effect of ageostrophy on the stability of vortices in a two-layer ocean. Ocean Mod. 23, 49–58.
Benilov, E.S., Sakov, P.V., 1999. On the linear approximation of velocity and density profiles in the problem of baroclinic instability. J. Phys. Oceanogr. 29, 1374–1381.
Boyd, J.P., 1985. Complex coordinate methods for hydrodynamic instabilities and Sturm-Liouville eigenproblems with an interior singularity. J. Comput. Phys. 57, 454–471.
Chelton, D.B., Schlax, M.G., Samelson, R.M., 2011. Global observations of nonlinear mesoscale eddies. Prog. Oceanogr. 91, 167–216.
Dewar, W.K., Gailliard, C., 1994. The dynamics of barotropically dominated rings. J. Phys. Oceanogr. 24 (1), 5–29.
Dritschel, D.G., Scott, R.K., Reinaud, J.N., 2005. The stability of quasi-geostrophic ellipsoidal vortices. J. Fluid Mech. 536, 401–421.
Dritschel, D.G., de la Torre Juárez, M., 1996. The instability and breakdown of tall columnar vortices in a quasi-geostrophic fluid. J. Fluid Mech. 328, 129–160.
Olson, D.B., 1991. Rings in the ocean. Annu. Rev. Earth Planet. Sci. 19, 283–311.
Pedlosky, J., 1987. Geophysical Fluid Dynamics, second ed. Springer.